Electronic Supplementary Information

Cream rolls-inspired advanced MnS/C composite for sodium-ion batteries: Encapsulating MnS creams into hollow N, S co-doped carbon rolls

Gaojie Li,[a] Kongyao Chen,*[a] Yanjie Wang,[a] Zhuo Wang,[a] Xueli Chen,[a] Siwen Cui,[a] Zijie Wu,[a,c] Constantinos Soutis,[c] Weihua Chen,*[b] Liwei Mi*[a]

[a] *Center for Advanced Materials Research, Zhongyuan University of Technology, Henan 450007, P. R. China*

[b] *College of Chemistry and Molecular Engineering, Zhengzhou University, Henan 450001, P. R. China*

[c] *The University of Manchester Aerospace Research Institute, University of Manchester, Manchester M13 9PL, United Kingdom*

* Corresponding author: *mlwzzu@163.com, chenweih@zzu.edu.cn, chenkongyao@zut.edu.cn.*

Experimental Section

Preparation of MnS/NSCTs composites. MnS/NSCTs composites were prepared by a simple freeze drying and heat treatment method. Firstly, 1.2 g $Mn(CH_3COO)_2{\cdot}4H_2O$ and 0.5 g cetyl trimethyl ammonium bromide (CTAB) were dissolved completely into 50 mL distilled water. Then, 1.0 g juncus was immersed into the solution and dried at 60°C overnight. After that, the precursor is freezed and dried for 24 h in a freeze dryer, then calcinated at 700°C for 5 h with the protection of N_2. Lastly, the samples were mixed with sulfur (weight ratios of 1:10) and calcinated at 500°C for 3 h with the protection of N_2, then MnS/NSCTs composites were achieved. Pure MnS are prepared via a similar way without the presence of juncus.

Material characterization. X-ray diffraction (XRD) and *ex-situ* XRD patterns were obtained with Polycrystalline X-ray powder diffractometer (Ultima IV, Rigaku Corporation) with Cu-Kα radiation. The microstructures and energy dispersive X-ray maps were obtained by scanning electron microscopy (SEM, Zeiss Merlin Compact). X-ray photoelectron spectroscopy (XPS) and *ex-situ* XPS analysis was performed by an energy spectrometer (Thermo Scientific K-Alpha) Thermogravimetric (TG) analysis was obtained by a thermo analyzer (TG 209F1, NETZSCH) from 50 to 850°C with a heating rate of 10°C min^{-1} in air. The specific surface area and pore distribution were calculated by Barrett-Joyner-Halenda (BJH) method.

Electrochemical Measurements. MnS/NSCTs electrodes were prepared by mixing MnS/NSCTs composites, acetylene black, and Polyvinylidene Fluoride (PVDF) with a weight ratio of 7:2:1, and 1-methyl-2-pyrrolidone was selected as the

solvent. Then the slurry was uniformly coated onto a copper foil, and dried at 80°C for 8 h. After rolled by a roller press, the copper foil was cut into wafers with a diameter of 8 mm. The mass loading of the active material was about 1~2 mg cm^{-2}. The working electrodes were MnS/NSCTs electrodes, the counter electrodes were home-made Na slices, the electrolyte was 1 mol L^{-1} sodium trifluomethanesulfonate in diethylene glycol dimethyl ether ($NaCF_3SO_3$/DEGDME), and the separators were glass fiber filters (Whatman GF/D). Then CR-2032 coin cells were assembled in an Ar filled glove box. The galvanostatic charge-discharge test was carried out by a multichannel battery tester (LAND CT2001A, Wuhan), and all the specific capacities are based on the weight of MnS/NSCTs composite. The voltage range is 0.2~3.0 V, and the specific capacity is based on the total mass of MnS or MnS/NSCTs samples. The voltage range is chosen from a comprehensive consideration of high capacity and long life. The cyclic voltammetry (CV) test was performed by an electrochemical workstation (CHI 660e, chenhua, Shanghai), and the scan rate was 0.2 mV s^{-1} with a voltage range of 0.2~3 V. Electrochemical impedance spectrum (EIS) and *in-situ* EIS was performed by an electrochemical workstation (Zennium-pro, Germany, Zahner), and the frequency range was from 0.1 Hz to 100 kHz.

BET Results

The specific surface area and pore size distribution of MnS/NSCTs composite are investigated by BET test. In Fig. 2b, the isothermal absorption-desorption curves of MnS/NSCTs manifest an IV-type absorption isothermal feature[1, 2]. According to the pore size distribution, MnS/NSCTs sample shows a typical mesoporous feature with a specific surface area of 36.05 m^2 g^{-1}, and the average porous size is 3.74 nm. However, numerous cavities in the tubes may not be detected by BET because of their oversize diameter (2~4 μm).

TG Results

TG is performed to ascertain the component of MnS/NSCTs. As is shown in Fig. 2c, the little weight loss below 200°C is attributed to the evaporation of water in the sample. Whereafter, slight weight increase appears from 340°C to 400°C, which may result from the formation of Mn_3O_4 and $MnSO_4$. The weight loss between 420°C and 520°C corresponds to the oxidization of carbon tubes, and the weight loss between 600°C and 800°C may come from the formation of Mn_2O_3. According to the TG curve, the weight ratio of MnS is about 56.0% in the cream roll-like MnS/NSCTs sample.

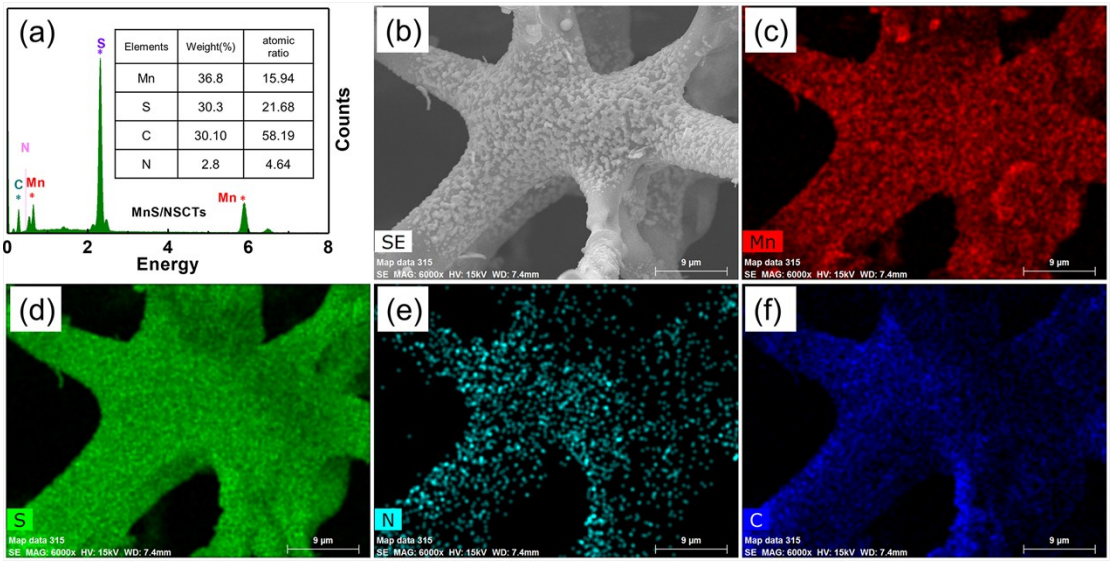

Fig. S1 Element analysis of MnS/NSCTs. (a) EDX; (b) morphology; (c) (d) (e) (f) mapping images of Mn, S, N and C.

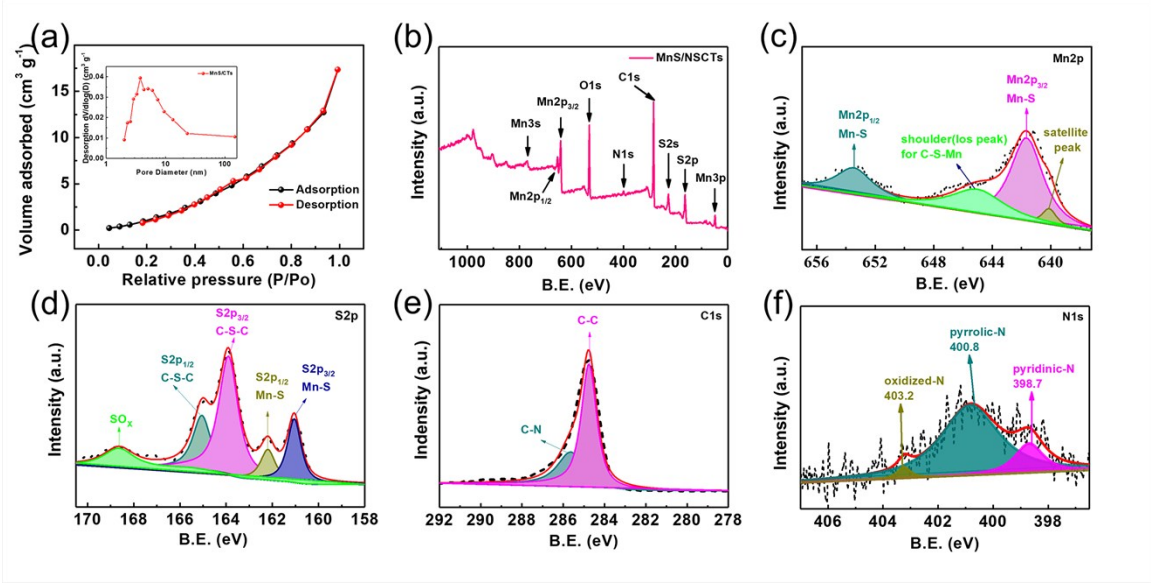

Fig. S2 BET and XPS of MnS/NSCTs. (a) Nitrogen adsorption-desorption curves and pore size distributions; (b) survey XPS spectrum of MnS/NSCTs; (c) (d) (e) (f) high-resolution XPS spectra of Mn, S, C and N. (a) XPS survey spectrum of MnS/NSCTs; (b) N1s spectrum of MnS/NSCTs.

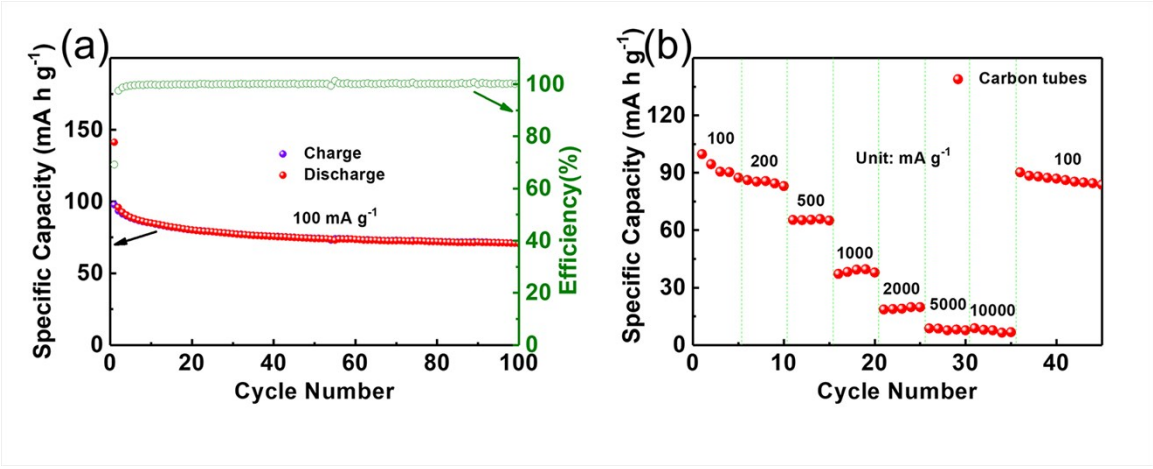

Fig. S3 Sodium storage performance of pure carbon from juncus. (a) Cycle performance; (b) rate performance.

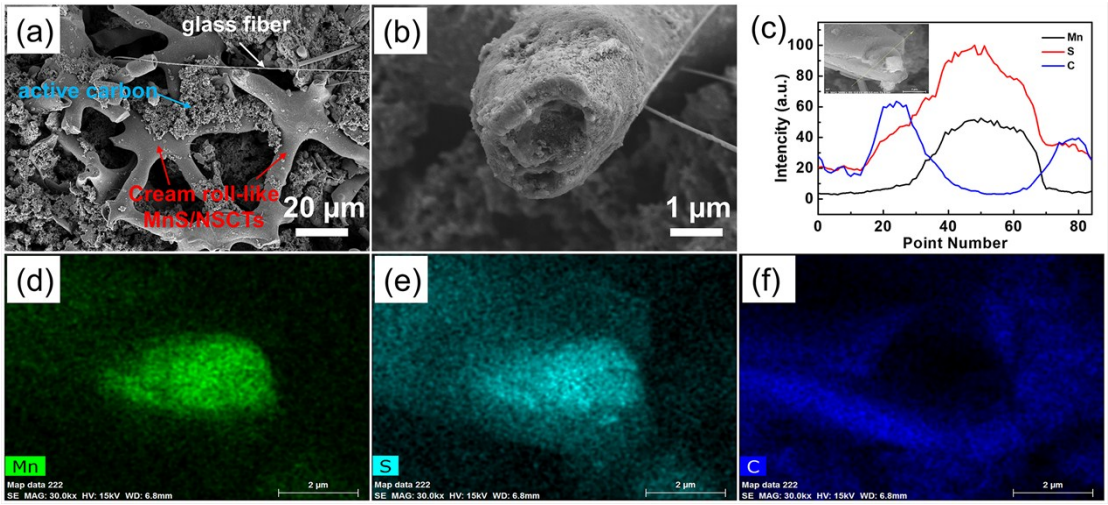

Fig. S4 Morphology and element distribution of MnS/NSCTs after 100 cycles. (a) (b) SEM images; (c) line scan results; (d) (e) (f) mapping images of Mn, S and C.

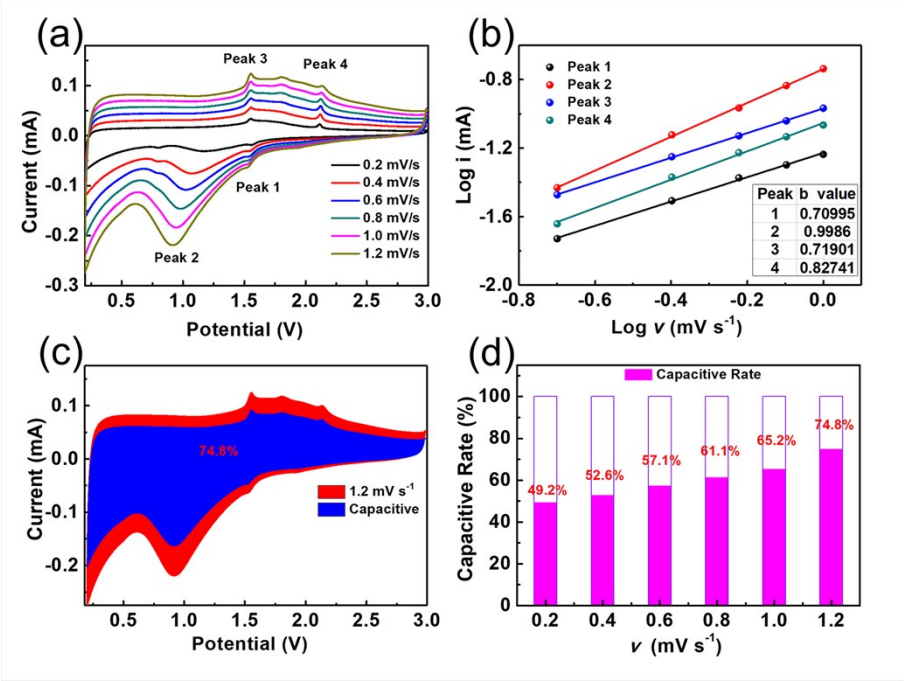

Fig. S5 CV test of MnS/NSCTs at various scan rates. (a) CV curves; (b) relationship of log *i* vs. log *v*; (c) capacitive capacity contribution at 1.2 mV s^{-1}; (d) capacitive capacity contribution at various scan rates.

References

1. S. Gao, G. Chen, Y. Dall'Agnese, Y. Wei, Z. Gao and Y. Gao, *Chemistry - A European Journal*, 2018, **24**, 13535-13539.
2. X. Xu, H. Zeng, D. Han, K. Qiao, W. Xing, M. J. Rood and Z. Yan, *ACS Appl. Mater. Interfaces*, 2018, **10**, 37172-37180.